



Size-dependent PM₁₀ indoor/outdoor/personal relationships for a wind-induced naturally ventilated airspace

Chung-Min Liao*, Jein-Wen Chen, Su-Jui Huang

Department of Bioenvironmental Systems Engineering, National Taiwan University, Taipei 10617, Taiwan, ROC

Received 1 December 2002; received in revised form 2 April 2003; accepted 2 April 2003

Abstract

We applied a simple size-dependent indoor air quality model associated with a compartmental lung model to characterize PM₁₀ indoor–outdoor–personal exposure relationships for wind-induced naturally ventilated residences in Taiwan region. The natural ventilation rate was quantified by the opening effectiveness for sidewall opening (SP) and covered ridge with sidewall opening (CRSP) type homes. The predicted PM₁₀ mass indoor/outdoor (I/O) ratios were 0.15–0.24 and 0.20–0.32, respectively, for SP and CRSP type homes. Results demonstrate that PM₁₀ I/O ratios for a wind-induced naturally ventilated airspace depend strongly on the ambient PM size distributions, building openings design (e.g. height to length ratio of openings and roof slope), wind speed and wind angle of incidence. The predictions from our lung model agreed favorable with the experimental deposition profiles in extrathoracic (ET), bronchial–bronchiolar (BB), and alveolar–interstitial (AI) regions. Our results demonstrate that ET region has higher PM₁₀ mass lung/indoor ratios (for north Taiwan region: 0.67–0.78; for central: 0.66–0.74) than that of BB (for north: 0.36–0.57; for central: 0.33–0.47) and AI regions (for north: 0.05–0.35; for central: 0.02–0.22). The present approach can be used in the future to appraise the significance of inter-subject lung morphology and breathing physiology variability for PM deposition and dose calculations.

© 2003 Elsevier Science Ltd. All rights reserved.

Keywords: Particulate matter; Deposition; Natural ventilation; Opening effectiveness; Indoor–outdoor–personal exposure; Lung; Modeling

1. Introduction

Outdoor particulate matters (PMs) present on the surface of streets may consist of a complex mixture of soil dust, deposited motor vehicle exhaust particles, tire dust, brake lining wear dust, plant fragments, and other biological materials. Pope and Dockery, 1992; Dockery et al. (1993); Schwartz (1993); Seaton et al. (1995); Ackermann-Lieblich et al. (1997) in their epidemiological studies indicated that the PMs in outdoor air were strongly associated with lung function parameters, respiratory symptoms and mortality. These findings were especially pronounced for inhaled thoracic parti-

cles (particles of aerodynamic equivalent diameter (AED) < 10 μm, PM₁₀).

Outdoor PM attributable to the indoor air in urban/suburban residence houses has been the most serious indoor air pollution in Taiwan region (Yang et al., 1999; Chen et al., 1999; Li and Lin, 2002). The relationship between exposure to airborne PM and resulting health effects is the subject of an ever-increasing number of studies. Guo et al. (1999) revealed that PM₁₀ was positively associated with the prevalence of asthma in middle-school students in Taiwan. Hwang and Chan (2002) demonstrated that rates of daily clinic visits were associated with current-day concentrations of PM₁₀ in Taiwan region.

In the indoor environment, the removal of entrained outdoor PMs occurs through ventilation and deposition. Natural ventilation is widely used in Taiwan region with

*Corresponding author. Tel.: +886-2-2363-4512; fax: +886-2-23-62-6433.

E-mail address: cmliao@ccms.ntu.edu.tw (C.-M. Liao).

the advantages of saving energy, expense, and installation time in that dwelling houses are controlled by natural convection to remove excessive heat and moisture. The mechanism of natural ventilation depends on wind effects, thermal buoyancy and the combination of both wind and buoyancy forces. Wind speed and wind direction are the dominant factors for wind-induced effects (Miguel et al., 2001). The characteristics of openings affect natural ventilation efficiency with the arrangement, location, and control of ventilation openings to achieve a desired ventilation rate and good distribution of ventilation air through the buildings.

In a naturally ventilated airspace, Brownian and turbulent diffusion, sedimentation, and laminar as well as convective flow exist to varying degrees and lead to particle deposition onto walls and other surfaces. Depending on the flow regime, different models have been proposed for particle deposition in a ventilated airspace. In the present work, we adopted a mathematical model derived by Crump and Seinfeld (1981) for the rate of aerosol deposition in a turbulence mixing enclosure of arbitrary shape under the assumption of homogeneous turbulent near the surfaces.

Numerous mathematical models for predicting PM deposition in the human airways have been developed over the years (Martonen and Zhang, 1993; ICRP, 1994; Lazaridis et al., 2001). In this present study, we employed an approach based on the concept of applying compartmental modeling to the human lung anatomy incorporated with the ICRP66 recommended model (ICRP, 1994). Numerous compartmental models have been proposed, differing in the representation of the tracheo-bronchial tree, the breathing physiology and resulting airflow, and the expressions used for calculating PM deposition efficiencies (Koblinger and Hofmann, 1990; Martonen and Zhang, 1993). In this present study, the main features of PM deposition mechanisms in lung include turbulent and Brownian diffusion, inertial impaction, interception, gravitational settling, and clearance as suggested by ICRP66 (ICRP, 1994).

Because the epidemiological literature has focused on health effects associated with ambient particle levels, we do not include indoor source in our analysis and focus on the PM₁₀ indoor/outdoor/lung (I/O/L) relationships. In this study, we attempt to understand the PM₁₀ I/O/L relationships focusing on the building operational characteristics of a wind-induced naturally ventilated airspace and the size-dependent effects on indoor PM₁₀ levels. We employed an opening effectiveness model to quantify the wind-induced natural ventilation for side-wall openings (SP) and covered ridge with sidewall openings (CRSP) that are commonly employed in Taiwan region. We predicted the size-dependent I/O/L ratios of PM₁₀ mass for urban and suburban naturally ventilated homes and compared our results with empirical evidence. There are uncertainties in the

measurements; thus, we also performed uncertainty analysis for the proposed model.

2. Materials and methods

2.1. Modeling PM I/O ratio for a naturally ventilated airspace

Thatcher and Layton (1995); Abt et al. (2000); Riley et al. (2002) have developed rigorous indoor air quality models for studying the PM I/O relationships and size-dependent removal mechanisms in a residence, in which the model employed by them applied also to our study. Combining the physical processes controlling the gain and loss rates, the deposition (including Brownian and turbulent diffusive deposition and gravitational sedimentation), and air exchange, yields a dynamic equation that describes the concentration profile of PM I/O relationships in a wind-induced naturally ventilated airspace.

Followed by the principle of mass balance under an isothermal condition in that resuspension, coagulation of particles, and phase change processes are neglected, the dynamic equation varying with particle size range k and time t are given by

$$\frac{dC_1(k, t)}{dt} = -(\lambda_n + \lambda_d(k))C_1(k, t) + \lambda_n C_o(k, t),$$

$$k = 1, 2, \dots, N - 1, \quad (1)$$

where $C_1(k, t)$ is the time-dependent indoor PM concentration in the k th size range (kg m^{-3}); $C_o(k, t)$ is the time-dependent outdoor PM concentration in the k th size range (kg m^{-3}); λ_n is the air exchange rate of natural ventilation through open windows and doors (h^{-1}) in which $\lambda_n = Q_n/V$, Q_n is the natural ventilation rate ($\text{m}^3 \text{h}^{-1}$); V is the air volume (m^3); $\lambda_d(k)$ is the deposition rate of indoor PM due to Brownian and turbulent diffusive deposition and gravitational sedimentation in the k th size range (h^{-1}); k is the size range number; and N is assigned to be the end point number for a k th size range, d_k and d_{k+1} .

The particles are divided into geometrically equal sized bins in the size range of interest. The PM concentration is assumed to be a constant aerodynamic equivalent diameter (AED) within each bin size. The end points, d_k and d_{k+1} , of the k th bin size are considered to be equal to the geometric mean of the end points of the bin size as

$$d_k = d_{\min} + \frac{(d_{\max} - d_{\min})(k - 1)}{N - 1},$$

$$k = 1, 2, \dots, N, \quad (2)$$

where particles smaller than d_{\min} (the minimum diameter) are considered to be the finest, and d_{\max} is the largest particle size of interest.

The C–S model is a well-established general model for the rate of aerosol deposition due to turbulent diffusion, Brownian diffusion, and gravitational sedimentation in a turbulently mixed arbitrary shape of airspace. Detailed derivation of the deposition model can be found in Liao et al. (2001).

Inhaled PMs deposit in the human airways by different deposition mechanisms, depending to varying extent on PM size, local airflow field, and lung architecture. Calculation of PM deposition is required to evaluate the size resolved loss term in Eq. (4). Turbulent diffusion, Brownian diffusion, inertial impaction, interception, gravitational settling, and PM clearance are the PM deposition mechanisms addressed in this study. The main features of the PM deposition model in the naturally ventilated airspace and in the human respiratory tract are listed in Table 1. Table 2 gives the input values of lung physiological parameters and deposition rate parameters used in the PM I/O models for naturally ventilated airspace and lung.

2.4. Opening effectiveness model

The natural ventilation rate (Q_n) depends on the effect of wind moving through openings. ASHRAE (1997) suggests an empirical expression to predict the flow through a sidewall opening as a function of wind speed and opening effectiveness as $Q_n = EA V_w$ where E is the opening effectiveness (dimensionless), A is the area of inlet opening (m^2), and V_w is the wind velocity ($m s^{-1}$). The traditional Buckingham Pi theorem is commonly used to derive an empirical relationship between opening effectiveness and variables in terms of dimensionless parameters. The dimensionless parameters selected in the present study include: (i) the Reynolds number (Re) defined by the opening length, air density, air velocity, and absolute air viscosity; (ii) the ratio between opening height and opening length (h_0/l_0); (iii) the incidence angle of wind flow (ϕ); and (iv) the slope of roof (θ). Detailed algorithm for developing the opening effectiveness model can be found in Yu et al. (2002). The expressions of opening effectiveness for the SP and CRSP type buildings, E_{SP} and E_{CRSP} , respectively, can be obtained as follows (Yu et al., 2002):

$$E_{SP} = 7.44 \times (0.2Re)^{-0.3495} (4h_0/l_0)^{0.1029} \times (\sin \phi)^{0.7524} (\sin \theta)^{-0.1486}, \quad (6)$$

$$E_{CRSP} = 33.81 (0.4Re)^{-0.3940} (3.2h_0/l_0)^{0.101} \times (\sin \phi)^{0.8799} (\sin \theta)^{1.0388}. \quad (7)$$

Table 3 gives the configuration parameters used in the present study for determining opening effectiveness for the SP and the CRSP type buildings located at north, central and south Taiwan region in that monthly

Table 1

Rate equations of PM deposition for naturally ventilated airspace and for human respiratory tract

Naturally ventilated airspace

$$\lambda_d(k) = \frac{1}{d_{k+1} - d_k} \int_{d_k}^{d_{k+1}} \lambda_d(d_p) d(d_p), \quad (T.1)$$

Where

$$\lambda_d(d_p) = \frac{1}{lwh} \left\{ (2wh + 2hl) \left(\left(\sin \frac{\pi}{n} \right) \times \left(k_e D(d_p)^{n-1} \right)^{1/n} \right) + wlv_s(d_p) \times \coth \left(\frac{\pi v_s(d_p)}{2 \left(n \sin \frac{\pi}{n} \right) \left(k_e D(d_p)^{n-1} \right)^{1/n}} \right) \right\}, \quad (T.2)^a$$

$$D(d_p) = \frac{k_B TC_{slip}}{3\pi\eta_a d_p}, \quad (T.3)^b$$

$$v_s(d_p) = \frac{\rho_p g d_p^2}{18\eta_a} C_{slip} \left(1 - \frac{\rho_a}{\rho_p} \right). \quad (T.4)^b$$

Slip correlation factor:

$$C_{slip} = \left(1 + \frac{\lambda}{d_p} \left(2.541 + 0.8 \exp \left(-0.55 \frac{d_p}{\lambda} \right) \right) \right). \quad (T.5)^b$$

Human respiratory tract^c

$$\lambda_{di}(d_p) = \frac{8}{D_i} \sin \frac{\pi}{n} \left(k_e D(d_p)^{n-1} \right)^{1/n}, \quad (T.6)^a$$

$$\lambda_{si}(d_p) = \frac{4v_s(d_p)}{D_i} \coth \left(\frac{\pi v_s(d_p)}{2 \left(n \sin \frac{\pi}{n} \right) \left(k_e D(d_p)^{n-1} \right)^{1/n}} \right), \quad (T.7)^a$$

$$\lambda_{imi}(d_p) = \frac{\rho_p d_p^2 C_{slip} g}{9\eta_a D_i} = Stk \frac{g}{U_i}, \quad (T.8)^b$$

Where Stk = Stokes number

$$e_i(d_p) = \frac{(1 - \alpha) (n_i / \sum n_i) d_p / D_i}{Ku(1 + d_p / D_i)}. \quad (T.9)^b$$

Kawabara number:

$$Ku = -\frac{\ln \alpha}{2} - \frac{3}{4} + \alpha - \frac{\alpha^2}{4}. \quad (T.10)^b$$

See Table 2 for description of symbols.

^a Derived from Crump and Seinfeld (1981).

^b Adopted from Hinds (1999).

^c The integrated formula for the k th bin is the same as Eq. (T.1).

Table 2
Input parameters used in the PM I/O model simulations for ventilated airspace and for lung

| Parameter | Description | Representation values |
|--|---------------------------------|---|
| Lung physiological parameters ^a | | |
| Q | Breathing rate (light exercise) | $1.2 \text{ m}^3 \text{ h}^{-1}$ |
| Q_f | Breathing frequency | $15 \text{ breaths min}^{-1}$ |
| V_t | Tidal volume | 1.331 |
| D_1, D_2, D_3 | Diameter of airways | 2.8, 0.53, 0.05 cm |
| n_1, n_2, n_3 | Number of airways | 1, 6.55×10^4 , 4.5×10^7 |
| V_1, V_2, V_3 | Volume of compartments in lung | 92.32, 94.6, 1580.4 cm^3 |
| Deposition rate parameters | | |
| N | Exponent constant | 2 ^b |
| k_c | Turbulent intensity parameter | $0.1 \text{ s}^{-1\text{c}}$ |
| k_B | Boltzmann's constant | $1.38 \times 10^{-16} \text{ dyn cm}^\circ \text{C}^{-1\text{d}}$ |
| T | Ambient temperature | 25°C |
| η_a | Dynamic viscosity of air | $1.85 \times 10^{-4} \text{ g cm}^{-1} \text{ s}^{-1\text{d}}$ |
| λ | Mean free path of air | $0.66 \times 10^{-5} \text{ cm}^\text{d}$ |
| ρ_a | Air density | $1.18 \times 10^{-3} \text{ g cm}^{-3\text{d}}$ |
| ρ_p | Particle density | $1.0 \text{ g cm}^{-3\text{d}}$ |

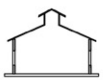
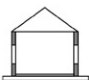
^a Adapted from ICRP66 (ICRP, 1994).

^b Adapted from Nazaroff et al. (1990).

^c Adapted from Nazaroff et al. (1990) and Nazaroff and Cass (1989).

^d Adapted from Hinds (1999).

Table 3
Configuration parameters used to determine opening effectiveness for SP and CRSP type buildings

| Building type | Volume V (m^3) | Height to length ratio (h_0/l_0) | Roof slope angle (θ) |
|---|-----------------------------|--------------------------------------|-------------------------------|
| CRSP type | | | |
|  | 256 | 2/3 | 23.5° |
| SP type | | | |
|  | 256 | 1/3 | 30° |

averaged data of wind speed and wind direction were obtained from Taiwan EPA.

2.5. Outdoor PM characteristics

The outdoor PM_{10} concentrations data of north, central, and south Taiwan region were obtained from

Taiwan EPA dated from November 1993 to May 2002 to evaluate the PM_{10} I/O ratio in naturally ventilated airspaces for SP and CRSP type buildings. We selected urban area located at north Taiwan (Taipei) region and suburban area located at central Taiwan (Taichung) region as study sites to evaluate the lung/indoor PM_{10} relationships in residence homes. The general urban site represents normal urban conditions without any specific air pollution sources, whereas the suburban site represents the industrial area and the air quality mainly contributed by mobile sources. The ambient particle concentrations were collected in the periods of April–October 2002 in that the field 24 h samples were continuously collected over a weeklong period in the monitoring month. We conducted a chamber test to verify the particle size distributions of the outdoor PM samples.

A portable laser dust monitor (Series 1100, Grimm Labortechnik GmbH & Co. KG, Ainring, Germany; referred to as DM1100) was used to analyze the PM characteristics. DM1100 combines the principles of aerodynamic particle size separation and light scattering particle detection. The particles can range from 0.5 to $10 \mu\text{m}$ AED. DM1100 measures mass concentrations in the range of $1.0\text{--}50,000 \mu\text{g cm}^{-3}$. Before the measurements, the DM1100 was calibrated with known particles of Uniform Latex Microspheres Polystyrene ($0.5 \mu\text{m}$) and Polymer Microspheres Styrene Vinyltoluene ($3 \mu\text{m}$) (Duke Scientific, Palo Alto, CA).

Results demonstrate that the particle size distributions of outdoor PM followed a lognormal distribution with a geometric mean diameter (GMD) of $1.06 \mu\text{m}$ and a geometric standard deviation (GSD) of 2.62 for north region and a GMD $4.32 \mu\text{m}$ and a 2.12 GSD for central region (Table 4). Table 4 summarizes the information of integrated number and mass concentrations for outdoor PM_{10} and indoor PM_{10} for SP and CRSP type buildings. We divided the two size ranges from 0.1 to $5 \mu\text{m}$ and 0.1 to $10 \mu\text{m}$ into 5 geometrically average size bins based on Eq. (2), in which the particle concentration in each bin size was also calculated. Generally, the CRSP type buildings have higher integrated number and mass concentrations than that of the SP type homes (Table 4).

2.6. Uncertainty analysis

Because of limitations in the data and theories to support PM I/O modeling in naturally ventilated airspace and in HRT, there is a need to characterize uncertainty and variability in the model approach and input parameters. We applied a Monte Carlo approach to appraise the impact of parameter uncertainty on our proposed PM I/O models. To express uncertainty in outdoor PM concentration, opening effectiveness, and PM I/O ratio parameters, we employed the Kolmogorov–Smirnov (K–S) statistics to optimize

Table 4

The characteristics of the outdoor and indoor PM₁₀ in north and central Taiwan region

| | North | Central |
|---|--|--------------------------------|
| Outdoor PM ₁₀ | | |
| Particle size distribution | LN(1.0 ⁶ μm, 2.62) ^a | LN(4.32 μm, 2.12) ^a |
| Integrated number concentration (m ⁻³) | 1.36 × 10 ⁶ | 5.09 × 10 ⁶ |
| Integrated mass concentration (μg m ⁻³) | 9.24 × 10 ⁻¹ | 27.7 |
| Indoor PM ₁₀ | | |
| SP type | | |
| Integrated number concentration (m ⁻³) | 0.33 × 10 ⁶ | 0.74 × 10 ⁶ |
| Integrated mass concentration (μg m ⁻³) | 2.26 × 10 ⁻¹ | 5.02 |
| CRSP type | | |
| Integrated number concentration (m ⁻³) | 0.44 × 10 ⁶ | 1.02 × 10 ⁶ |
| Integrated mass concentration (μg m ⁻³) | 2.98 × 10 ⁻¹ | 5.54 |

^aLN(GMD, GSD): Lognormal distribution with geometric mean diameter (GMD) and geometric standard deviation (GSD).

the goodness-of-fit of distributions. We employed @RISK (Version 4.5, Professional Edition, Palisade Corp., USA) to analyze data and to estimate distribution parameters. Results from goodness-of-fit statistics suggest that the normal distribution model fits the observed data. To test the convergence and stability of the numerical output, we performed independent runs at 1000, 4000, 5000, and 10 000 iterations with each parameter sampled independently from appropriate distribution at the start of each replicate. For this study, 5000 iterations are sufficient to ensure stability of results. We employed 95th-percentile predictions of indoor PM₁₀ level as our conservatism values to calculate the PM₁₀ L/I ratio for each lung compartment.

3. Results and discussion

3.1. PM₁₀ I/O relationships in naturally ventilated airspace

The outdoor and indoor PM₁₀ mass concentrations for SP and CRSP type buildings are presented in Fig. 1A. Box and whisker plots are used to represent the uncertainty in that boxes show 25th and 75th percentiles and whiskers are 5th and 95th percentiles. The relatively lower variability was observed in indoor PM₁₀ mass. Median values of measured outdoor PM₁₀ mass concentrations were 55.42, 64.06, and 86.94 μg m⁻³, respectively, in north, central, and south Taiwan region. The CRSP type building has higher calculated indoor PM₁₀ mass concentrations (median 11.17–19.65 μg m⁻³) than that of the SP type building (median 8.05–14.36 μg m⁻³). The CRSP type buildings have higher PM₁₀ mass I/O ratios (median 0.17–0.27) than that of SP type buildings (median 0.13–0.20) (Fig. 1B). Strength of the I/O relationships for PM₁₀ mass for SP and CRSP

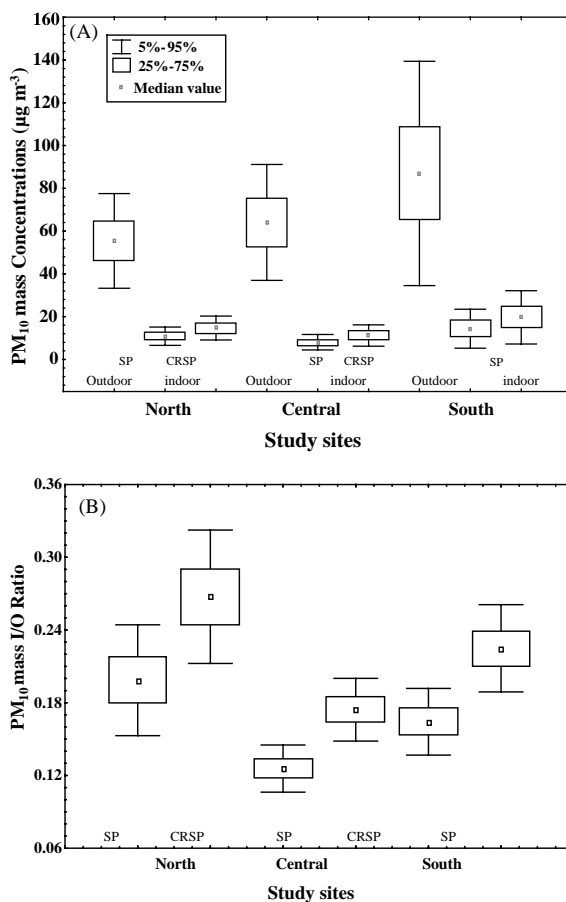


Fig. 1. (A) Calculated indoor PM₁₀ mass concentrations and (B) calculated PM₁₀ mass indoor/outdoor (I/O) ratio for SP and CRSP type buildings in the north, central, and south Taiwan region. Box and whisker plot shows the uncertainty.

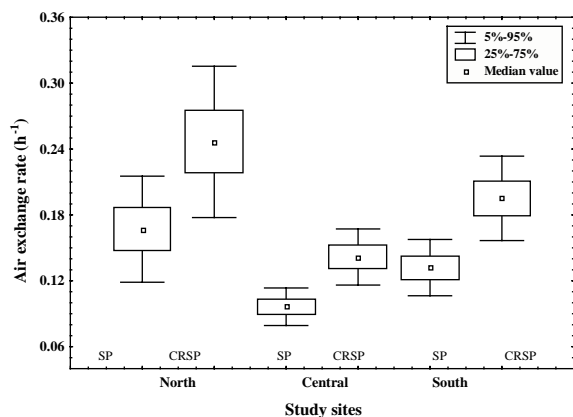


Fig. 2. Air exchange rates of SP and CRSP type buildings in the north, central, and south Taiwan region.

type buildings in different Taiwan region is partly explained by the natural ventilation rates of the buildings (Fig. 2). Fig. 2 indicates that in all regions, CRSP type building has higher air exchange rate (median 0.14–0.25 h⁻¹) than that of SP type building (median 0.1–0.17 h⁻¹). Little studies containing suitable data were identified, thus extremely limited empirical evidence was available for model validation, especially for the wind-induced naturally ventilated residences in Taiwan region.

In our work, average deposition rate for PM₁₀ was calculated to be 0.67 ± 0.2 h⁻¹. This deposition rate is equivalent to a deposition velocity of 0.54 m h⁻¹ corresponding to a surface-to-volume of 1.25 m⁻¹ in this present study. Wallace (1996) reported that an average deposition rate for PM₁₀ was found to be 0.65 h⁻¹, indicating that their fitted PM₁₀ deposition rate is consistent with that employed in this study. We suggest that a mathematical relationship among indoor/outdoor concentrations of PM, air exchange rates, deposition velocity, sources, and sinks of PM can be developed. Furtaw et al. (1996) demonstrated that the amount of turbulence in a room is proportional to the air exchange rate. Accordingly, an increase in turbulence will increase the particle deposition rate (Crump and Seinfeld, 1981; Nazaroff and Cass, 1989). These factors will lead to the increase in deposition velocity for all particle sizes as air exchange rate increases.

In a single residence study, Thatcher and Layton (1995) calculated deposition velocities between 0.64 and 4.15 m h⁻¹ for 1 to 6 μm AED particles. In several residences, Fogh et al. (1997) measured particle deposition velocities between 0.18 and 1.1 m h⁻¹ for particle AED between 0.5 and 5.5 μm in that calculated I/O mass concentration ratios varied between 0.1 and 0.7 for the same sized particles. In an enclosed chamber, Lewis (1995) experimentally measured deposition rates

between 0.25 and 1.1 h⁻¹ for particle AED between 1 and 7 μm. Lewis (1995) also demonstrated that increasing the pressure differential or aperture of an opening increased the penetration for all particle sizes. Riley et al. (2002) used deposition rates ranged from 0.17 to 2.1 h⁻¹ PM₁₀ to estimate the PM mass I/O ratios.

The linear fits between measured outdoor and simulated indoor PM₁₀ mass concentrations in SP and CRSP type buildings in Fig. 3 indicate that, for all cases, fitted linear models give good correlations between fitted and simulated indoor PM₁₀ mass concentrations, where r^2 ranged from 0.70 to 0.97 ($p < 0.05$, average $r^2 = 0.86$), indicating the PM₁₀ mass concentrations in the indoor air were dominated by outdoor sources. This also implied that 70–97% (or 86%, on average) of the variation of the indoor PM₁₀ mass concentrations was explained by the outdoor concentrations of PM₁₀. For the SP and CRSP type buildings in north, central, and south Taiwan region, the intercepts were not different from zero at 95% confidence and the slopes were in good agreement with the PM₁₀ mass I/O ratios in the 5th- and 95th-percentiles range (Figs. 1 and 3). Larger scattering of the data was observed in north Taiwan region where the air exchange rates had higher variability than that of in central and south region (Fig. 2).

The average residential exposure to outdoor PM₁₀ can also be estimated from the least-squares linear regression of indoor concentrations on outdoor concentrations performed for homes without strong indoor sources (Fig. 3). When the intercept is equal to zero, the slope of the regression indicates that the average percent of the outdoor PM₁₀ that penetrate indoors. In north Taiwan homes, the indoor PM₁₀ mass concentrations were 19 ± 3% ($r^2 = 0.73 ± 0.03$) of the outdoor concentrations. In central and south region homes, the indoor concentrations of PM₁₀ were 15 ± 2.5% ($r^2 = 0.89 ± 0.01$) and were 20 ± 3% ($r^2 = 0.96 ± 0.005$) of outdoor concentrations, respectively.

3.2. PM₁₀ I/O relationships in HRT

We compared our theoretical predictions to independently published experimental data obtained from ICRP66 (ICRP, 1994) and other different studies (Yu and Diu, 1983; Sarangapani and Wexler, 2000; Hofmann et al., 2000; Lazaridis et al., 2001; Asgharian et al., 2001; Schroeter et al., 2001; Salma et al., 2002; Hofmann et al., 2002) that referred to as Non-ICRP66 (Fig. 4). Table 5 summarizes the data set obtained from ICRP66 and Non-ICRP66 used to test the proposed deposition model. The experimental data were obtained from considered very reliable data. Model predictions agree favorable with the experimental deposition profile in the ET, BB, and AI regions (Fig. 4), even though the experimental data are quite scattered, owing to

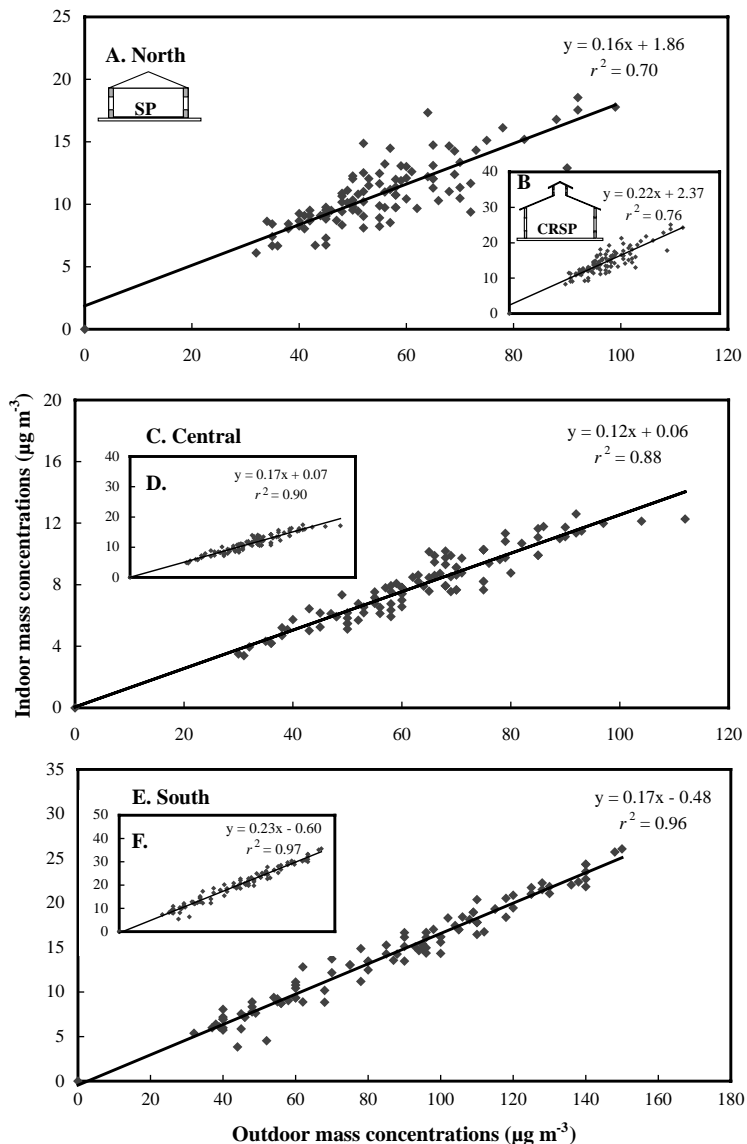


Fig. 3. Fitted linear correlation between outdoor (measured) and indoor (simulated) PM_{10} mass concentrations for SP (A, C, E) and CRSP (B, D, F) type buildings in the north, central, and south Taiwan region.

non-consistency in methodology and to parameter variability. The increase in deposition with increasing PM size for the size range considered in Fig. 4 is in agreement with predictions of the ICRP66 and Non-ICRP66. The comparisons between predicted and measured lung deposition profiles suggest that the model seems to be adequate in describing the upper and lower deposition bounds. The close agreement of the present lung model with the experimental data also suggests that the model captures the underlying nature of the physiochemical processes responsible for PM deposition in the HRT.

Personal exposure in CRSP type buildings has higher PM deposition in HRT than that of in SP type buildings

(Fig. 5). Different PM_{10} number distribution patterns in lung regions in north and central Taiwan region (Fig. 5) resulted partly from different PM size distributions (Table 4). The dominant deposition mechanism in the lung regions was found to be the inertial impaction rate, in which the ranged order of magnitude were 10^{-2} – 10^{-1} and 10^{-2} – $10^0 s^{-1}$, respectively, for the north and central Taiwan region. Generally, the region AI has higher deposition rates than that of in regions ET and BB. The lung region ET has higher PM_{10} mass lung/indoor (L/I) ratios (for north Taiwan region: 0.67–0.78; for central: 0.66–0.74) than that of lung regions BB (for north: 0.36–0.57; for central: 0.33–0.47) and AI (for north:

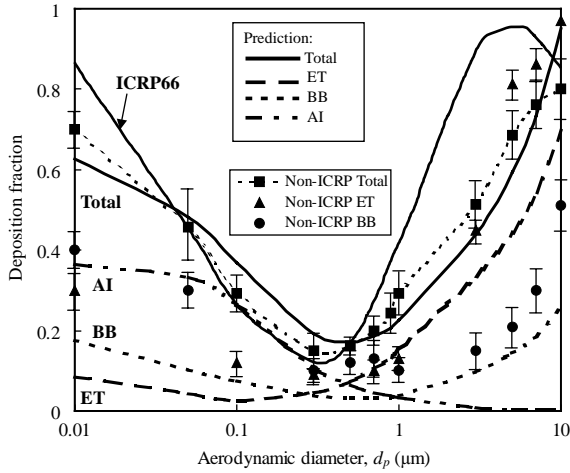


Fig. 4. Comparison of extrathoracic (ET), bronchial-bronchiolar (BB), and alveolar-interstitial (AI) regions deposition data from ICRP66 and non-ICRP66 with theoretical predictions. Model parameters include branching angle of 45° , tidal volume of 1330 cm^3 , and breathing frequency of 15 min^{-1} with initial PM size distribution of a geometric mean diameter $1.06 \mu\text{m}$ and a geometric standard deviation 2.62.

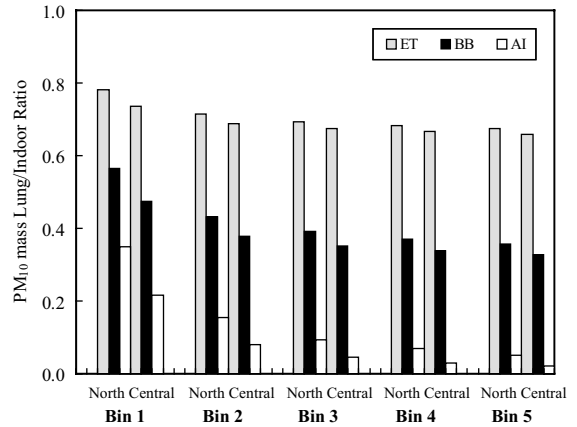


Fig. 6. Calculated PM_{10} mass lung/indoor (L/I) ratios for each size bin in lung regions ET, BB, and AI in the north and central Taiwan region.

0.05–0.35; for central: 0.02–0.22) for each bin size in that larger bin sizes has smaller PM_{10} mass L/I ratios (Fig. 6). The SP and CRSP type buildings have similar distribution patterns of PM_{10} mass L/I ratio (Table 4).

Our proposed simple lung model provides an easy way to account for and keep track of the contribution of different processes of lung deposition profiles, even though our model is based on many idealized assumptions such as one-dimensional airflow and single morphological change. Our approach can also examine independently the processes and mechanisms that govern the inhalation route of the exposure-dose-response scenario.

4. Conclusions

Our results demonstrate that PM_{10} mass indoor/outdoor (I/O) ratios can vary from 0.15–0.24 and 0.20–0.32 (95th-percentiles) for SP and CRSP type homes, respectively. In north Taiwan homes, the indoor PM_{10} mass concentrations were 19% of the outdoor concentrations. In central and south region homes, the indoor concentrations of PM_{10} were 15% and 20% of outdoor concentrations, respectively.

Comparison of human respiratory tract (HRT) deposition data from ICRP66 and Non-ICRP66 with our theoretical predictions, results show that predictions are agreement with the experimental deposition profiles in lung regions, even though experimental deposition data show considerable scatter. Generally, personal exposure in CRSP type buildings has higher PM

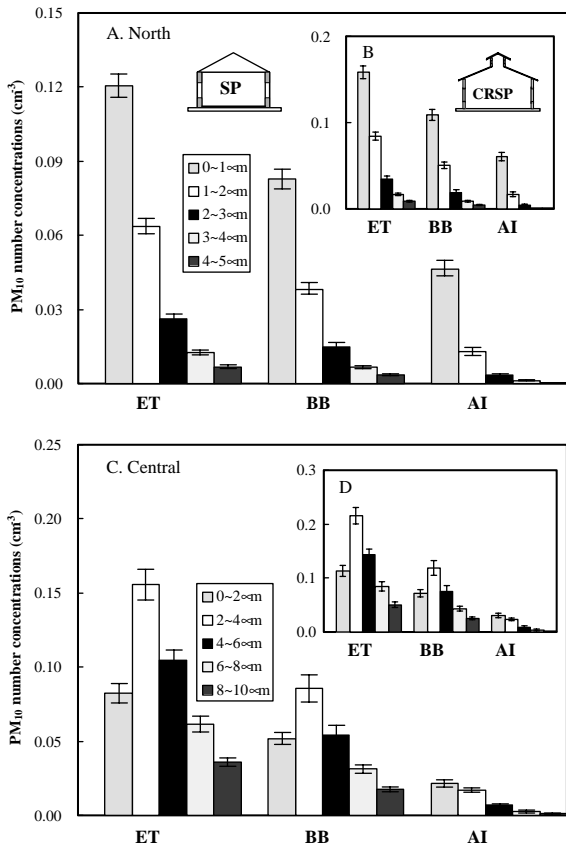


Fig. 5. PM_{10} number concentrations of each size range in lung regions ET, BB, and AI for SP (A, C) and CRSP (B, D) type buildings in the north and central Taiwan region. Error bars show one standard deviation from the mean.

Table 5

Data set of the deposition fraction obtained from published literature used to test the deposition model

| | Particle diameter (μm) | | | | | | | | | | | |
|-------------------------------|-------------------------------------|------|------|------|------|------|------|------|-------|-------|-------|-------|
| | 0.01 | 0.05 | 0.1 | 0.3 | 0.5 | 0.7 | 0.9 | 1.0 | 3.0 | 5.0 | 7.0 | 10.0 |
| <i>ICRP66</i> | 0.86 | 0.45 | 0.27 | 0.13 | 0.17 | 0.28 | 0.38 | 0.42 | 0.90 | 0.96 | 0.93 | 0.85 |
| <i>Non-ICRP66 total</i> | | | | | | | | | | | | |
| Yu and Diu (1983) | 0.73 | 0.40 | 0.25 | 0.14 | 0.16 | 0.22 | 0.26 | 0.25 | 0.55 | 0.70 | 0.76 | 0.77 |
| Sarangapani and Wexler (2000) | 0.66 | 0.52 | 0.33 | 0.19 | 0.16 | 0.19 | 0.21 | 0.33 | 0.52 | 0.65 | 0.72 | 0.76 |
| Asgharian et al. (2001) | 0.74 | 0.46 | 0.29 | 0.12 | 0.18 | 0.19 | 0.24 | 0.28 | 0.45 | 0.73 | 0.80 | 0.87 |
| Mean | 0.71 | 0.46 | 0.29 | 0.15 | 0.17 | 0.20 | 0.24 | 0.29 | 0.51 | 0.69 | 0.76 | 0.80 |
| S.D. | 0.04 | 0.07 | 0.04 | 0.04 | 0.01 | 0.02 | 0.03 | 0.04 | 0.05 | 0.04 | 0.04 | 0.06 |
| <i>Non-ICRP66 ET</i> | | | | | | | | | | | | |
| Sarangapani and Wexler (2000) | 0.36 | | 0.15 | 0.11 | | 0.16 | | 0.17 | 0.49 | 0.85 | 0.87 | 0.98 |
| Schroeter et al. (2001) | 0.32 | | 0.10 | 0.07 | | 0.11 | | 0.15 | 0.44 | 0.79 | 0.81 | 0.95 |
| Salma et al. (2002) | 0.27 | | 0.13 | 0.09 | | 0.14 | | 0.12 | 0.42 | 0.76 | 0.78 | 0.98 |
| Mean | 0.31 | | 0.12 | 0.09 | | 0.14 | | 0.13 | 0.45 | 0.82 | 0.86 | 0.97 |
| S.D. | 0.05 | | 0.03 | 0.02 | | 0.03 | | 0.03 | 0.04 | 0.04 | 0.04 | 0.02 |
| <i>Non-ICRP66 BB</i> | | | | | | | | | | | | |
| Hofmann et al. (2000) | 0.41 | 0.34 | | 0.12 | 0.13 | 0.15 | | 0.11 | 0.17 | 0.24 | 0.37 | 0.55 |
| Asgharian et al. (2001) | 0.38 | 0.31 | | 0.09 | 0.09 | 0.09 | | 0.08 | 0.12 | 0.17 | 0.30 | 0.51 |
| Lazaridis et al. (2001) | 0.36 | 0.38 | | 0.07 | 0.11 | 0.13 | | 0.08 | 0.11 | 0.18 | 0.30 | 0.45 |
| Hofmann et al. (2002) | 0.45 | 0.32 | | 0.12 | 0.11 | 0.16 | | 0.13 | 0.18 | 0.23 | 0.33 | 0.53 |
| Mean | 0.39 | 0.32 | | 0.10 | 0.12 | 0.13 | | 0.11 | 0.15 | 0.21 | 0.33 | 0.51 |
| S.D. | 0.05 | 0.05 | | 0.02 | 0.03 | 0.04 | | 0.03 | 0.04 | 0.04 | 0.04 | 0.05 |
| <i>Predictions</i> | | | | | | | | | | | | |
| Total | 0.63 | 0.48 | 0.37 | 0.19 | 0.17 | 0.19 | 0.21 | 0.23 | 0.44 | 0.60 | 0.73 | 0.95 |
| ET | 0.09 | 0.04 | 0.03 | 0.05 | 0.07 | 0.11 | 0.13 | 0.15 | 0.33 | 0.44 | 0.54 | 0.70 |
| BB | 0.18 | 0.10 | 0.08 | 0.04 | 0.03 | 0.03 | 0.04 | 0.04 | 0.10 | 0.15 | 0.19 | 0.25 |
| AI | 0.37 | 0.33 | 0.26 | 0.11 | 0.07 | 0.05 | 0.04 | 0.04 | 0.009 | 0.006 | 0.005 | 0.004 |

The predictions obtained from present model are also shown (see Fig. 4).

deposition in HRT than that of in SP type buildings. The dominant deposition mechanism in the lung regions was found to be the inertial impaction rate, in which the ranged order of magnitude was 10^{-2} – 10^0 s^{-1} . Our results demonstrate that extrathoracic region has higher PM_{10} mass lung/indoor (L/I) ratios (0.66–0.78) than that of bronchial–bronchiolar region (0.33–0.57) and alveolar–interstitial region (0.02–0.35). We may apply this present model to predict the dose resulting from exposure from inhalation to airborne PM such as fine diesel PM, fugitive dust, and bioaerosols and to analyze clinical data and protocols in the field of aerosol therapy.

References

- Abt, E., Suh, H.H., Catalano, P., Koutrakis, P., 2000. Relative contribution of outdoor and indoor particle sources to indoor concentrations. *Environment Science and Technology* 34, 3579–3587.
- Ackermann-Lieblich, U.A., Leuenberger, Ph., Schwartz, J., Schindler, C., Monn, C., Sapaldia, T., 1997. Lung function and long term exposure to air pollutions in Switzerland. *American Journal of Respiratory and Critical Care Medicine* 155, 122–129.
- Asgharian, B., Hofmann, W., Bergmann, R., 2001. Particle deposition in a multi-path model of the human lung. *Aerosol Science and Technology* 34, 332–339.
- ASHRAE, 1997. *Handbook of Fundamentals*, Atlanta Ga, American Society of Heating, Refrigerating and Air Conditioning Engineers.
- Chen, M.L., Mao, I.F., Lin, I.K., 1999. The $\text{PM}_{2.5}$ and PM_{10} particles in urban area of Taiwan. *The Science of the Total Environment* 226, 227–235.
- Crump, J.G., Seinfeld, J.H., 1981. Turbulent deposition and gravitational sedimentation of an aerosol in a vessel of arbitrary shape. *Journal Aerosol Science* 12, 405–415.
- Dockery, D.W., Pope, C.A., Xu, X.P., Spengler, J.D., Ware, J.H., Fay, M.E., Ferris, B.G., Speizer, F.E., 1993. An association between air pollution and mortality in 6 United States. *New England Journal of Medicine* 329, 1753–1759.
- Fogh, C.L., Byrne, M.A., Roed, J., Goddard, A.H., 1997. Size specific indoor aerosol deposition measurements and derived I/O concentrations ratios. *Atmospheric Environment* 31, 2193–2203.
- Furtaw, E.J., Pandian, M.D., Nelson, D.R., Behar, J.V., 1996. Modeling indoor air concentrations near emission sources

- in imperfectly mixed rooms. *Journal of the Air and Waste Management Association* 46, 861–868.
- Guo, Y., Lin, Y.C., Sung, F.C., Huang, S.L., Ko, Y.C., Lai, J.S., Su, H.J., Shaw, C.K., Lin, R.S., Dockery, D.W., 1999. Climate, traffic-related air pollutants, and asthma prevalence in middle-school children in Taiwan. *Environmental Health Perspectives* 107, 1001–1006.
- Hinds, W.C., 1999. *Aerosol Technology: Properties, Behavior, and Measurement of Airborne Particles*, 2nd Edition. Wiley, New York.
- Hofmann, W., Bergmann, R., Balásházy, I., 2000. Variability and inhomogeneity of radon progeny deposition patterns in human bronchial airways. *Journal of Environmental Radioactivity* 51, 121–136.
- Hofmann, W., Asgharian, B., Winkler-Heil, R., 2002. Modeling intersubject variability of particle deposition in human lungs. *Journal of Aerosol Science* 33, 219–235.
- Hwang, J.S., Chan, C.C., 2002. Effects of air pollution on daily clinic visits for lower respiratory tract illness. *American Journal of Epidemiology* 155, 1–10.
- ICRP, 1994. Human respiratory tract model for radiological protection, a report of a task group of the International Commission on Radiological Protection, ICRP Publication No. 66. Elsevier, New York.
- Koblinger, L., Hofmann, W., 1990. Monte-Carlo modeling of aerosol deposition in human lungs 1. Simulation of particle-transport in a stochastic lung structure. *Journal of Aerosol Science* 21, 661–674.
- Lazaridis, M., Broday, D.M., Hov, Ø., Georgopoulos, P.G., 2001. Integrated exposure and analysis system. 3: deposition of inhaled particles in the human respiratory tract. *Environmental Science and Technology* 35, 3727–3734.
- Lewis, S., 1995. Solid particle penetration into enclosure. *Journal of Hazardous Materials* 43, 195–216.
- Li, C.S., Lin, C.H., 2002. PM_{10} / $PM_{2.5}$ / PM_{10} characteristics in the urban atmosphere of Taipei. *Aerosol Science and Technology* 36, 469–473.
- Liao, C.M., Chen, J.W., Huang, M.Y., Chen, J.S., Chang, T.J., 2001. An inhalation dose model for assessing dust-borne VOC-odor exposure from feeding in swine buildings. *Transactions of the ASAE* 44, 1813–1824.
- Martonen, T.B., Zhang, Z., 1993. Deposition of sulfate acid aerosols in the developing lung. *Inhalation Toxicology* 5, 165–187.
- Miguel, A.F., van de Braak, N.J., Silva, A.M., Bot, G.P.A., 2001. Wind-induced airflow through permeable materials part II: air infiltration in enclosure. *Journal of Wind Engineering and Industrial Aerodynamic* 89, 59–72.
- Nazaroff, W.W., Cass, G.R., 1989. Mass-transport aspects of pollution removal at indoor surface. *Environment International* 15, 567–584.
- Nazaroff, W.W., Ligocki, M.P., Ma, T., Cass, G.R., 1990. Particle deposition in museums: comparison of modeling and measurement results. *Aerosol Science and Technology* 13, 332–348.
- Pope, C.A., Dockery, D.W., 1992. Acute health effects of PM_{10} pollution on symptomatic and asymptomatic children. *American Review of Respiratory Disease* 145, 1123–1128.
- Riley, W.J., McKone, T.E., Lai, A.K., Nazaroff, W.W., 2002. Indoor particulate matter of outdoor origin: importance of size-dependent removal mechanisms. *Environment Science and Technology* 36, 200–207.
- Salma, I., Balásházy, I., Winkler-Heil, R., Hofmann, W., Záray, G., 2002. Effect of particle mass size distribution on the deposition of aerosols in the human respiratory system. *Journal of Aerosol Science* 33, 119–132.
- Sarangapani, R., Wexler, A.S., 2000. The role of dispersion in particle deposition in human airways. *Toxicological Science* 54, 229–236.
- Schroeter, J.D., Musant, C.J., Hwang, D., Burton, R., Guilmette, R., Martonen, T.B., 2001. Hygroscopic growth and deposition of inhaled secondary cigarette smoke in human nasal pathways. *Aerosol Science and Technology* 34, 137–143.
- Schwartz, J., 1993. Particulate air pollution and chronic respiratory disease. *Environment Research* 62, 7–13.
- Seaton, A., MacNee, W., Donaldson, K., Godden, D., 1995. Particulate air pollution and acute health effects. *Lancet* 345, 176–178.
- Thatcher, T.L., Layton, D.W., 1995. Deposition, resuspension, and penetration of particles within a residence. *Atmospheric Environment* 29, 1487–1497.
- Wallace, L., 1996. Indoor particles: a review. *Journal of the Air and Waste Management Association* 46, 98–126.
- Yang, H.H., Chiang, C.F., Hee, W.J., Hwang, K.P., Wu, E.M., 1999. Size distribution and dry deposition of road dust PAHs. *Environment International* 25, 585–597.
- Yu, C.P., Dju, C.K., 1983. Total and regional deposition of inhaled aerosols in humans. *Journal of Aerosol Science* 14, 599–609.
- Yu, H., Hou, C.H., Liao, C.M., 2002. Scale model analysis of opening effectiveness for wind-induced natural ventilation openings. *Biosystems Engineering* 82, 199–207.